



LAWRENCE
LIVERMORE
NATIONAL
LABORATORY

Solid-Solid Phase Transition Kinetics of FOX-7

A. K. Burnham, R. K. Weese, R. Wang, Q. S. M.
Kwok, D. E. G. Jones

July 18, 2005

2005 NATAS Annual Conference
Universal City, CA, United States
September 18, 2005 through September 21, 2005

Disclaimer

This document was prepared as an account of work sponsored by an agency of the United States Government. Neither the United States Government nor the University of California nor any of their employees, makes any warranty, express or implied, or assumes any legal liability or responsibility for the accuracy, completeness, or usefulness of any information, apparatus, product, or process disclosed, or represents that its use would not infringe privately owned rights. Reference herein to any specific commercial product, process, or service by trade name, trademark, manufacturer, or otherwise, does not necessarily constitute or imply its endorsement, recommendation, or favoring by the United States Government or the University of California. The views and opinions of authors expressed herein do not necessarily state or reflect those of the United States Government or the University of California, and shall not be used for advertising or product endorsement purposes.

Solid-Solid Phase Transition Kinetics of FOX-7*

Alan K. Burnham^a, Randall K. Weese^a, Ruiping Wang^b, Queenie S. M. Kwok^b
and David E. G. Jones^b

^aLawrence Livermore National Laboratory, P. O. Box 808, Livermore,
California 94551-0808, U. S. A.

^bCanadian Explosives Research Laboratory, 555 Booth St., Ottawa, Ontario,
K1A 0G1, Canada
burnham1@llnl

ABSTRACT

Since it was developed in the late 1990s, 1,1-diamino-2,2-dinitroethene (FOX-7), with lower sensitivity and comparable performance to RDX, has received increasing interest. This paper will present our results for the phase changes of FOX-7 using DSC and HFC (Heat Flow Calorimetry). DSC thermal curves recorded at linear heating rates of 0.10, 0.35 and 1.0 °C min⁻¹ show two endothermic peaks and two exothermic peaks. The two endothermic peaks represent solid-solid phase transitions, which have been observed in the literature at 114 °C (β - γ) and 159 °C (γ - δ) by both DSC and XPD (X-ray powder diffraction) measurements. The first transition shifts from 114.5 to 115.8 °C as the heating rate increases from 0.10 to 1.0 °C min⁻¹, while the second transition shifts from 158.5 to 160.4 °C. Cyclical heating experiments show the endotherms and exotherms for a first heating through the γ phase to the δ phase, a cooling and reversion to the α or β phase, and a second heating to the γ and δ phases. The data are interpreted using kinetic models with thermodynamic constraints.

INTRODUCTION

Much effort has been devoted to an ongoing search for more powerful, safer and environmentally friendly explosives. Since it was developed in the late 1990s¹, 1,1-diamino-2,2-dinitroethene (FOX-7), with lower sensitivity than and comparable performance to RDX, has received increasing interest. Preliminary results on the physical and chemical characterization of FOX-7 have shown that it possesses good thermal and chemical stability.¹ It is expected that FOX-7 will be an important new ingredient in high performance, insensitive munition (IM) explosives.²

Our laboratories are interested in characterizing the properties of explosive materials by thermal analysis. In previous work, Östmark et al have reported that DSC curves of FOX-7 exhibit two minor endothermic peaks as well as two major exothermic peaks.³ Two endothermic peaks at ~116 and ~158 °C suggest the presence of two solid-solid phase transitions. A third phase change below 100 °C has also been reported based on a X-ray powder diffraction (XPD) study,⁴ but it has been attributed to improper crystallization (N. Latypov, personal communication, 2005). We present here our

*This work was conducted in part under the auspices of the U.S. Department of Energy by the University of California, Lawrence Livermore National Laboratory, under Contract number W-7405-Eng-48

experimental and kinetic analysis results for the phase changes of FOX-7 using DSC (Differential Scanning Calorimetry) and HFC (Heat Flow Calorimetry).

EXPERIMENTAL

FOX-7 (1,1-diamino-2,2-dinitroethene) used for HFC analyses was obtained from NEXPLO Bofors AB. For DSC measurements it was synthesized at LLNL by P. Pagoria.

DSC measurements were conducted using a TA Instrument model 2920 Differential Scanning Calorimeter and hermetically sealed aluminum pans with pinholes in the lids. Approximately 0.5 mg was decomposed at heating rates from 0.1 to 1.0 °C min⁻¹. Degradation was carried out under nitrogen carrier gas at a flow rate of 100 cm³ min⁻¹.

A modified SETARAM C-80 instrument was used for a HFC study on thermal decomposition of FOX-7. About 50 mg of FOX-7 was placed in an alumina liner which was loaded into a stainless steel vessel. An equivalent mass of sapphire was used as the reference material. The experiments were conducted at ambient and 8.85 MPa argon pressure and a heating rate of 0.3 °C min⁻¹ in a temperature range of 28 to 300 °C.

RESULTS AND DISCUSSION

Kinetic characteristics of the phase transitions are illustrated in Figures 1 and 2, which show the endotherms and exotherms for a first heating through the γ phase to the δ phase, a cooling and reversion to the α or β phase, and a second heating to the γ and δ phases. A large uncertainty in the phase transformation assignments is whether the broad feature that sometimes occurs during cooldown in the vicinity of 150 °C is a reversion from δ to γ or merely a baseline problem. It is possible that the reversion at 75 °C for cooling at °C min⁻¹ and at 50 °C at 30 °C min⁻¹ is a direct transformation from δ to α or β phase. The increase in reversion temperature with a decrease in heating rate is consistent with the previous observation of the reversion peaking at 102 °C for cooling at ~0.3 °C min⁻¹.

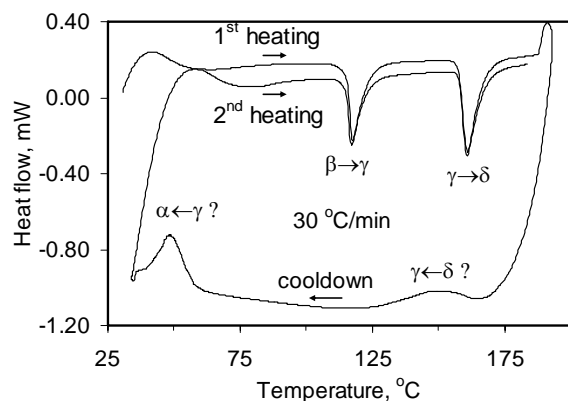


Figure 1. Cyclic heating and cooling of FOX-7 at 30 °C min⁻¹.

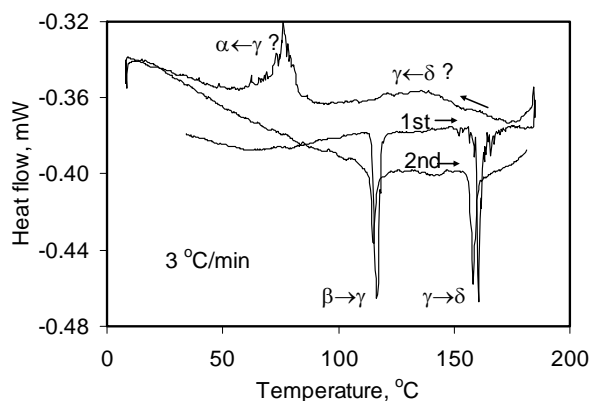


Figure 2. Cyclic heating and cooling of FOX-7 at 3 °C min⁻¹.

A summary of the temperature maxima and heats absorbed during the $\beta \rightarrow \gamma$ and $\gamma \rightarrow \delta$ transformations for virgin material heated at various rates is given in Table 2. There is a small increase in the peak temperature of the endotherm in each case. The standard deviations of the peak temperatures averaged 0.25 °C for $\beta \rightarrow \gamma$ and 0.7 °C for $\gamma \rightarrow \delta$, so the overall increase is far greater than the uncertainty at any given heating rate. There is no obvious dependence of absorbed heat on heating rate, and the average enthalpies were 21.6 J g⁻¹ for $\beta \rightarrow \gamma$ and 17.7 J g⁻¹ for $\gamma \rightarrow \delta$.

Table 2. Summary of phase transition data at multiple heating rates.

Hr, °C min ⁻¹	$\beta \rightarrow \gamma$		$\gamma \rightarrow \delta$	
	T _p , °C	ΔH, J g ⁻¹	T _p , °C	ΔH, J g ⁻¹
0.1	114.5	25.3	158.5	15.0
0.35	114.9	21.3	158.9	14.6
1.0	115.8	18.7	160.4	16.8
3.0	118.1	21.9	164.7	21.0
10	119.7	21.5	163.8	18.7
30	122.3	20.7	165.3	20.0

The transition profile changes markedly for the second heating, as shown in Figure 2. For the same heating rate of 3 °C min⁻¹, the reheat phase transition occurs at a lower temperature and with a smoother, narrower, conversion profile. By analogy to more detailed studies of the HMX $\beta \rightarrow \delta$ phase transition, the reaction profile of the original material is actually a superposition of nucleation events for individual crystallites. At low heating rates, the interfacial growth of the phase transition is fast relative to the nucleation probability, so the features are well resolved. The activation energy for interfacial growth is lower than that of nucleation, so the reaction profiles tend to smear together at higher heating rates. The reverted material has much finer crystal domain sizes. The smoothness of the conversion profile may be due to a tighter nucleation probability distribution for this finer grain size.

Similar results were obtained by HFC, as shown in Figure 3. The endotherm of the first heating agrees very well with that by DSC in Table 2, and the slight decrease in the transition temperature upon the second heating agrees with the DSC result in Figure 2. The temperature of the reversion exotherm follows the trend established by the two DSC experiments—the faster the heating rate, the greater amount of cooling prior to the reversion.

One method of determining kinetic parameters is Kissinger's method,⁵ in which the peak temperatures are plotted as a function of heating rate via the relationship

$$\ln(H_r/T_p^2) = -E/RT_p + \ln(AR/E). \quad (1)$$

Here, H_r is the heating rate, and the reaction rate constant k equals $Ae^{-E/RT}$. The plots are shown in Figure 4 for the two phase transitions. The slope gives E/R , and the intercept combined with the slope gives A . Such an analysis gives 850 kJ mol⁻¹ for $\beta \rightarrow \gamma$ and 1054 kJ mol⁻¹ for $\gamma \rightarrow \delta$, which are higher than is physically plausible.

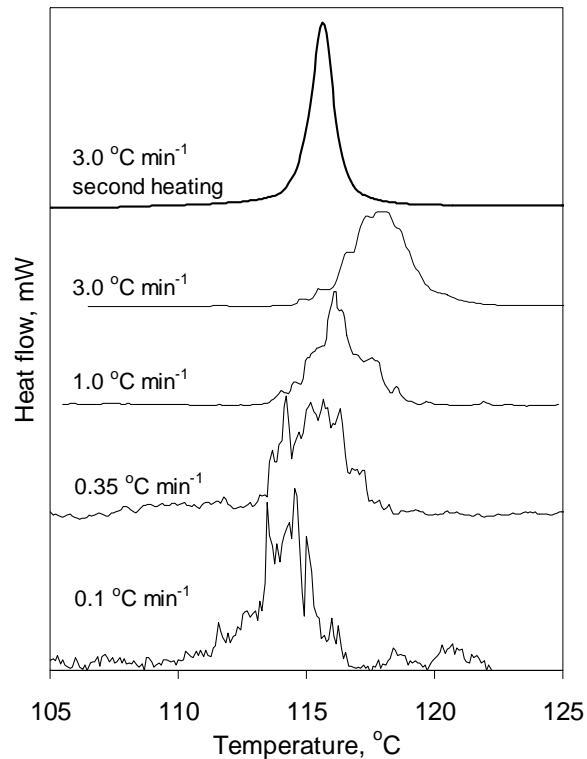


Figure 2. Change in the phase transition reaction profile as a function of heating rate and heating cycle. Endothermic heat flow is upwards in this plot.

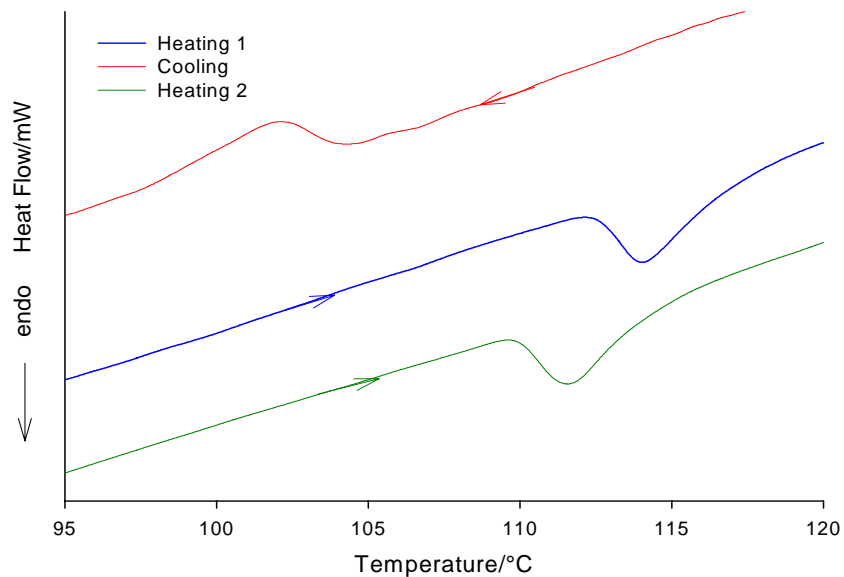


Figure 3. The HFC cyclic study on FOX-7 in the temperature range of 60-130 °C

This result is easy to understand if one considers the limit in which the phase transition occurs very rapidly as soon as the transition temperature is achieved. This limit gives a constant peak T and an infinite value for the activation energy. In fact, it is well known that the apparent activation energy by such a simple analysis approaches infinity

at the transition temperature, and two similar theories have been derived and applied to the $\beta \rightarrow \delta$ phase transition of HMX.^{6,7} The simplest way to think of this effect is that the effective rate constant equals the forward rate constant times a thermodynamic back-reaction factor of $1 - K_{eq}$, where $K_{eq} = K_o e^{-\Delta H/RT}$ is the equilibrium constant. Then

$$\frac{E_{eff}}{R} = -\frac{1}{k_{eff}} \frac{dk_{eff}}{d(1/T)} = \frac{E}{R} + \frac{\Delta H}{R} [K_{eq} - 1]. \quad (2)$$

Just as predicted, as the peak temperature approaches the $\beta \rightarrow \gamma$ transition temperature in Figure 4, the instantaneous slope and apparent activation energy approach infinity.

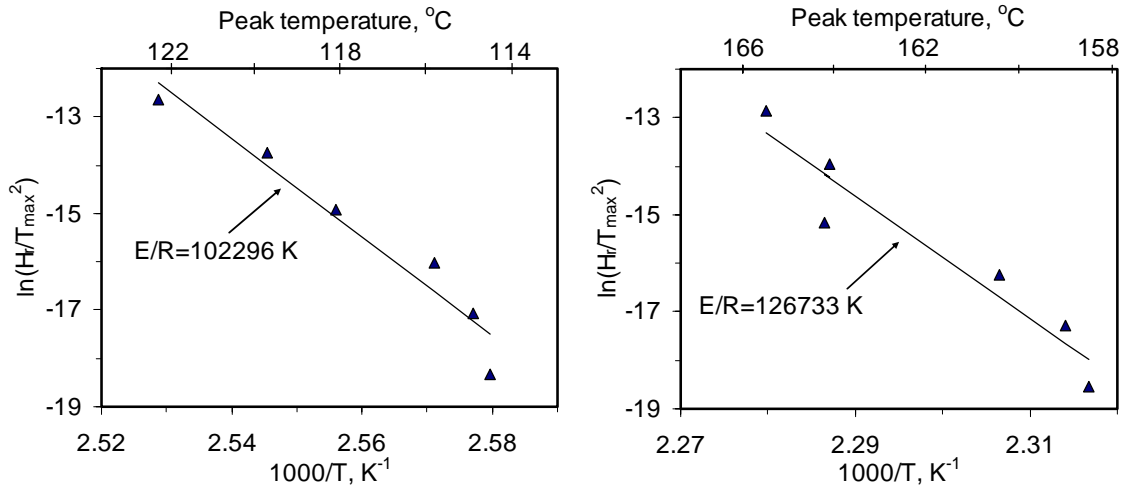


Figure 4. Kissinger kinetic analysis for the $\beta \rightarrow \gamma$ and $\gamma \rightarrow \delta$ phase transitions.

A better kinetic analysis approach is to use the equilibrium-inhibited Prout-Tompkins approach of Burnham et al.:

$$-dx/dt = kx^n(1-qx)^m(1-1/K_{eq}), \quad (3)$$

where x is the fraction unconverted, k is the rate constant, n is the reaction order, q is an initiation parameter, m is a nucleation-growth parameter, and K_{eq} is the equilibrium constant for the transition ($K=K_o e^{-\Delta H/RT}$). Comparisons of measured and calculated conversions are shown in Figures 5 and 6, respectively, for the β - γ and γ - δ phase transitions, and the model parameters are given in the figure captions.

In principle, ΔH can be taken from Table 2 and K_o calculated from the condition that $K=1$ at the transition temperature. However, such an approach did not work well for the $\beta \rightarrow \gamma$ phase transition. A much better fit to the data, shown in Figure 4, was obtained when K_o and ΔH were fitted as well as the Prout-Tompkins kinetics parameters using the LLNL Kinetics05 program. The resulting transition enthalpy is an order of magnitude greater than measured directly. The width of the transformation is underestimated at the lowest heating rate (probably because of a distribution of nucleation energies), and the induction time is underestimated at rapid heating rates. These characteristics could be fitted with a more detailed model. The same fitting procedure gave a value of ΔH for the $\gamma \rightarrow \delta$ transition that was about 25% larger than measured by DSC. On the other hand, the

activation energy and frequency factor are still higher than is physically plausible, although not quite as bad as those from the Kissinger analysis. These high values occur because a small temperature dependence for the thermodynamic inhibition term requires a higher temperature dependence of the forward kinetic rate. These results probably reflect both the inherent limitation of this approximate model and the sensitivity of the parameters to relatively small changes in the conversion profiles.

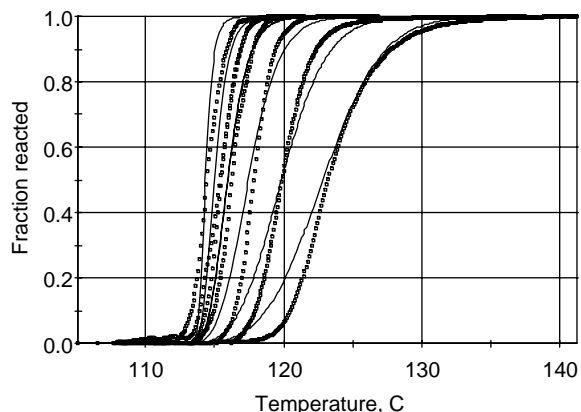


Figure 5. Measured and calculated fractions converted ($\beta \rightarrow \gamma$) at heating rates of 0.1, 0.35, 1.0, 3.0, 10, and 30 $^{\circ}\text{C min}^{-1}$ (left to right). The model parameters are $A=1.52 \times 10^{28} \text{ s}^{-1}$, $E=215.0 \text{ kJ mol}^{-1}$, $n=1.34$, $m=0.21$, $q=0.999$, $K_o=5.13 \times 10^5$, and $\Delta H=42.27 \text{ kJ mol}^{-1}$.

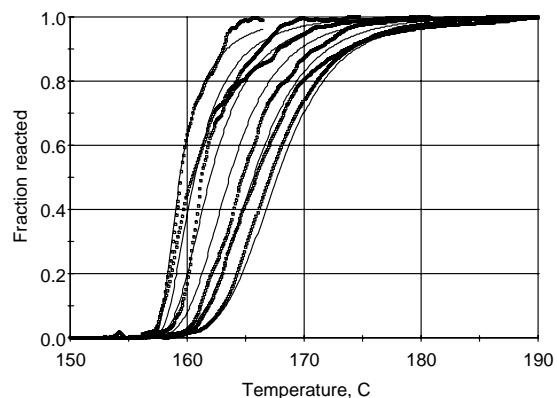


Figure 6. Measured and calculated fractions converted ($\gamma \rightarrow \delta$) at heating rates of 0.1, 0.35, 1.0, 3.0, 10, and 30 $^{\circ}\text{C min}^{-1}$ (left to right). The model parameters are $A=8.64 \times 10^{77} \text{ s}^{-1}$, $E=647.4 \text{ kJ mol}^{-1}$, $n=2.85$, $m=0.0$, $q=0.999$, $K_o=2.51$, and $\Delta H=3.298 \text{ kJ mol}^{-1}$.

A more detailed nucleation-growth model was also presented by Burnham et al.⁶ for the HMX phase transition. A comparison of calculated conversions with data are shown for that model in Figure 7, using parameters similar to those for HMX as prescribed in the figure caption. This model explicitly details both the nucleation and growth processes. It also allows a Weibull distribution of defect energies to account for the variation in nucleation times and temperatures above that expected for the statistical variation intrinsic to a kinetic process. In the current application, however, the Weibull parameters here were chosen to reflect a negligible defect energy and distribution. The high value of the nucleation activation energy is fixed by the breadth of the distribution of nucleation events at the fastest heating rate.

The back-reaction during cool down also has thermodynamic and kinetic aspects.⁸ The driving force for the reversion increases in proportion to the degree of undercooling, but the rate constant decreases exponentially with temperature. Consequently, the two factors work in opposite directions for reversion, while they work in concert for conversion. This accounts for the greater dependence of the peak temperature for reversion as a function of heating rate than for conversion.

The reaction model in Figure 7 is, in principle, reversible. Using the same parameters, the amount reverted at three heating rates is given in Figure 8. At the slowest heating rate, about half of the sample reverts between 110 and 80 $^{\circ}\text{C}$, with a maximum reversion rate at 105 $^{\circ}\text{C}$. At the fastest heating rate, the sample is kinetically frozen

before a significant amount of material can revert. At the faster rates, less reverts, but the temperature of maximum reversion rate is nearly the same.

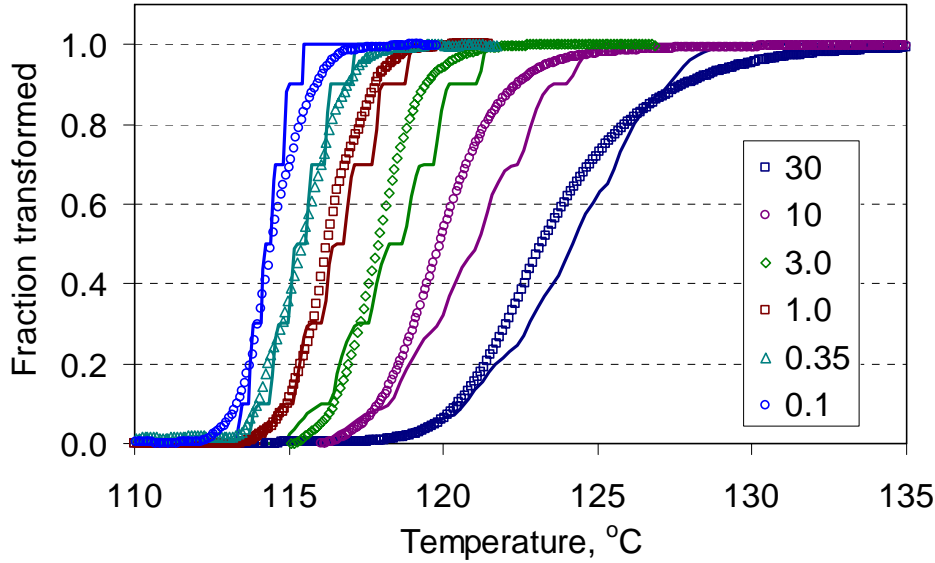


Figure 7. Comparison of measured and calculated transformations for the $\beta \rightarrow \gamma$ phase transition from 0.1 to 30 $^{\circ}\text{C}/\text{min}$ using the detailed nucleation-growth model of Burnham et al.⁶ The model used a forward nucleation rate of $7.0 \times 10^{47} e^{-40000/T} \text{ s}^{-1}$, a forward growth rate of $1.0 \times 10^6 e^{-2013/T} \mu\text{m s}^{-1}$, and an equilibrium coefficient of $2.705 e^{-384.17/T}$. The latter exponential corresponds to an enthalpy equal to that measured by DSC.

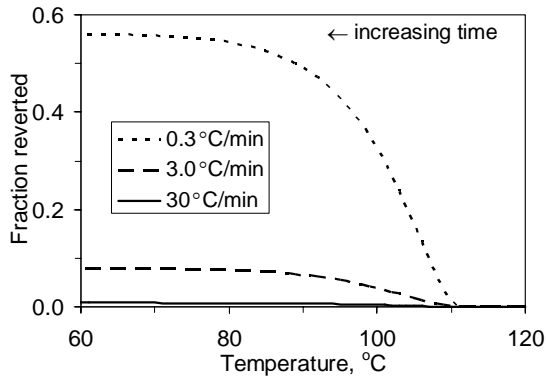


Figure 8. Cumulative amount of FOX-7 reverted to β phase as a function of temperature as the sample is cooled, as calculated in the kinetic model used in Figure 6.

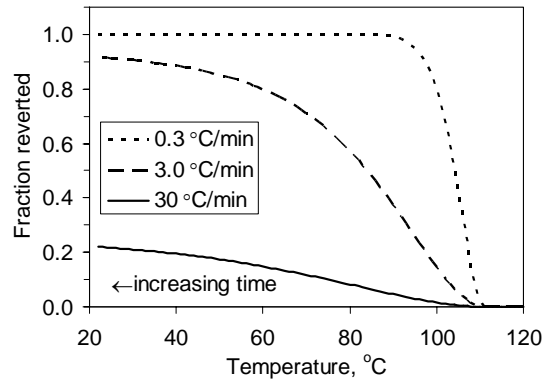


Figure 9. Cumulative amount of FOX-7 reverted to β phase as a function of temperature as the sample is cooled for a model in which the forward ($\beta \rightarrow \gamma$) nucleation rate is changed of $5.23 \times 10^3 e^{-4352/T} \text{ s}^{-1}$.

This result is fundamentally different than observed in the data, in which the temperature of maximum reversion rate decreases from ~ 102 $^{\circ}\text{C}$ at ~ 0.3 $^{\circ}\text{C min}^{-1}$ to ~ 75 $^{\circ}\text{C}$ at 3 $^{\circ}\text{C min}^{-1}$ to ~ 50 $^{\circ}\text{C}$ at 30 $^{\circ}\text{C min}^{-1}$. Furthermore, the reversion begins just below the phase transition temperature in all these cases, while the experimental evidence is that

essentially nothing happens until a significant time below the transition, which means an increasing drop in temperature as heating rate increases.

Part of the source of the discrepancy is in the extremely high value of the nucleation activation energy, which causes the reaction to be quenched rapidly as temperature decreases. In fact, one can achieve substantially higher amounts of reversion at all three heating rates and a decreasing maximum reversion rate with increased cooling rate by using a much lower activation energy. This is shown in Figure 9. Furthermore, the temperature of maximum reversion rate decreases from $\sim 105\text{ }^{\circ}\text{C}$ at $\sim 0.3\text{ }^{\circ}\text{C min}^{-1}$ to $\sim 94\text{ }^{\circ}\text{C}$ at $3\text{ }^{\circ}\text{C min}^{-1}$ to $\sim 82\text{ }^{\circ}\text{C}$ at $30\text{ }^{\circ}\text{C min}^{-1}$. This T_{max} trend is closer to what is observed, but the calculated temperature interval is still broad compared to what is observed.

A possible solution to this dilemma is to make the nucleation process itself a sequential reaction. Recall that the high activation energy is a result of constraining the nucleation events over a relatively narrow temperature range at high heating rates. A sequence of reaction steps with lower activation energy can accomplish the same thing. Furthermore, a sequential nucleation process would also show an induction period prior to reversion as is observed in the data.

A sequential process for nucleation is also attractive mechanistically. The formation of a stable nucleus probably results from the independent movement of several molecules in close proximity into a configuration that can support a growth interface. Although the thermodynamic probability of forming such a nucleus, or transition state, depends only on temperature, a multi-step mechanism would require an induction time before the first such nucleus is observed, and thereafter, the number of nuclei would increase with time according to the kinetics of the final step. Such a detailed model of nucleation growth has not yet been constructed, but it would appear to have the promise of resulting in more reasonable kinetic parameters for both the forward and reverse phase transitions.

REFERENCES

- ¹ H. Bergman, H. Ösmark, M-L. Pettersson, U. Bemm and M. Hihkiö, Some Initial Properties and Thermal Stability of FOX-7, *IM & EM Technol. Symp.*, 1999, 346.
- ² I. J. Lochert, FOX-7 - A New Insensitive Explosive, *DSTO*, 2001.
- ³ H. Östmark, H. Bergman, U. Bemm, P. Geode, E. Holmgren, M. Johansson, A. Langlet, N.V. Latypov, A. Pettersson, M-L. Pettersson, N. Wingborg, C. Vörde, H. Stenmark, L. Karlsson, M. Hihkiö, 2,2-Dinitro-ethene-1,1-diamine (FOX-7) – Properties, Analysis and Scale-up, *ICT*, 2001, 26-1.
- ⁴ U. Bemm and Lars Eriksson, Phase Transitions in FOX-7, *IM & EM Technol. Symp.*, 2001, 775-790.
- ⁵ H. E. Kissinger, Reaction Kinetics in Differential Thermal Analysis, *Anal. Chem.* 29, 1702-1706, 1957.
- ⁶ A. K. Burnham, R. K. Weese, B. L. Weeks, A Distributed Activation Energy Model of Thermodynamically Inhibited Nucleation and Growth Reactions and its Application to the β - δ Phase Transition of HMX, *J. Phys. Chem.* 108, 19432-19441, 2004.
- ⁷ B.F. Henson, L. Smilowitz, B. W. Asay, P. M. Dickson, The β - δ Phase Transition in the Energetic Nitramine Octahydro-1,3,5,7-tetranitro-1,3,5,7-tetrazocine: Thermodynamics, *J. Chem. Phys.* 117, 3780-3788, 2002.
- ⁸ J. D. Hoffman and R. L. Miller, Kinetics of crystallization from the melt and chain folding in polyethylene fractions revisited: theory and experiment, *Polymer* 38, 3151-3212, 1997.